Effect of Planform Aspect Ratio on Flow Oscillations in Rectangular Cavities

Peter J. Disimile
Associate Professor,
Department of Aerospace Engineering,
University of Cincinnati,
Cincinnati, OH 45221-0070

Norman Toy
Professor

Eric Savory
Lecturer,
Fluid Mechanics Research Group,
Department of Civil Engineering,
University of Surrey,
Guildford GU2 5XH, UK

An experimental investigation was undertaken to examine the effect of cavity lateral width on the flow oscillations that occur in an open cavity placed within a turbulent subsonic boundary layer. A rectangular cavity with a length to depth ratio L/D=1 and planform aspect ratio L/W=0.115 was placed within a thick turbulent boundary layer with a corresponding $Re_\theta = 10.5 \times 10^3$. *Pressure time histories were acquired at six separate cavity widths (or L/W values) using microphone-type pressure transducers. The spectral character of these signals was analyzed and the pressure levels and dominant frequencies determined. This study indicates that large changes in the pressure level occur as L/W varies from 0.115 to 0.682. A state of fluid dynamic resonance was observed at L/W =0.137 and fluid–acoustic resonance at L/W=0.682, the smallest cavity width. Relative sound pressure level calculations indicate that the energy within the cavity compared with that of the boundary layer, was observed to increase by approximately 40 percent at L/W=0.137.* [S0098-2202(00)00601-5]

Introduction

The flow over and around surface cutouts or cavities immersed in a boundary layer can cause large fluctuations in the flow parameters, such as pressure, velocity, and density, as well as providing a source of strong propagating acoustic waves. Such fluctuations may give rise to local changes in drag, damage to surface mounted instruments, or structural failure due to resonance. Hence, cavity flows are of interest in many branches of engineering.

The flow field surrounding rectangular cavities contains a mixture of unsteady flow regimes, namely, unstable shear layers that shed vortices in coherent patterns, pressure waves, and resident vortices (provided that the longest axis of the cavity is oriented in the spanwise direction). The location of the separating shear layer and the generation of self-sustaining oscillations depend upon conditions both inside and outside the cavity and this, in turn, influences the internal and external flow fields. This interaction is a result of an extremely complicated flow pattern that appears to depend upon the shape of the cavity, Mach number, Reynolds number, and the turbulence characteristics of the approaching boundary layer [1]. In the case of cavities with relatively small streamwise length to depth (L/D) ratios the shear layer spans the cavity opening and this is classified as an ''open'' flow regime. For longer cavities the ''closed'' flow regime occurs where the shear layer attaches onto the cavity base.

Although the mechanism by which flow is induced into the cavity, together with the resulting acoustic oscillations, have been studied by many investigators, a complete analysis has, so far, not been possible. One potential model for describing the interaction between the induced flow and the acoustic oscillations was suggested by Rossiter [2] in which he described how vortices that are shed periodically from the upstream lip of the cavity convect downstream and impinge on the aft wall of the cavity, thereby generating an acoustic wave. These acoustic disturbances propagate upstream and, upon reaching the forward lip of the cavity, cause the shear layer to separate, resulting in the shedding of a new vortex. In this way the vortex and the acoustic disturbances form a feedback loop. However, Plumblee et al. [3] proposed that the observed tones were solely a result of cavity acoustic resonance and that the frequency of these tones corresponded to the maximum acoustic response of the cavity. In contrast, Block [4] described a feedback mechanism based on the interaction of the separated shear layer with the boundaries of the cavity, in a manner similar to that suggested by Rossiter [2].

Although many of the cavities that have been studied were rectangular in cross section, each had a different aspect ratio, with only a few investigations involved in evaluating the frequency and amplitude content of the cavity as its width W was altered [4–6]. As a result, the extent to which the cavity aspect ratio influences either the frequency and/or the amplitude of these oscillations is still a subject of uncertainty. Of those studies, East [5] concluded that the span of the cavity did not appear to significantly effect the observed cavity oscillation phenomena, and suggested that the cavity resonance was fluid dynamically induced. This, it was stated, was the result of tuned amplification being produced by the unsteadiness of the shear layer edge tone, coupled with the cavity enclosure acting as an acoustic resonator.

In a later study by Block [4] it was noted that for cavities with the same L/D ratio the responses for both wide and narrow cutouts (cavities) peaked at the same frequency. However, although the resonant frequency was not related to the cavity width, the narrower cavities (that is, those with higher L/W ratios) produced larger and more sharply defined peaks when compared to the wider cavities. Furthermore, since the depth of their cavity was maintained constant it was also concluded that, due to the location of the peaks remaining unaltered with width, the frequency of the resonance was mostly dependent on the length of the cavity L. However, this work provided further evidence that the quality factor Q, the ratio of the center frequency/bandwidth of the peaks, of the cavity response appeared to be inversely proportional to the width W. Hence, it was deduced that narrow cavities have a high Q rating and will require higher velocities before oscillations may begin. However, they will still maintain some tonal spectra at lower velocities. Indeed, based on Block's examination of different length/width ratios of $L/W=0.541$ and 1.0 for a constant length/depth ratio of $L/D=1.0$, it was concluded that as the width W decreased (or L/W increased) the sound pressure level (SPL) and quality factor Q both increased.

In a more recent aeroacoustic study by Ahuja and Mendoza [6]

Contributed by the Fluids Engineering Division for publication in the JOURNAL OF FLUIDS ENGINEERING. Manuscript received by the Fluids Engineering Division December 21, 1998; revised manuscript received October 4, 1999. Associate Technical Editor: P. Bearman.

the effect of cavity width on flow oscillations was again examined. From their studies they reported the following salient features:

(a) The frequency of the peak oscillation was unaffected by changes in cavity width.
(b) Cavity noise reductions of up to 15 dB were noted for three-dimensional cavities.
(c) As $L/W=1.0$ was approached, the amplitude of the cavity tones reached an asymptote.
(d) The farfield broadband noise was reduced with decreasing cavity width.

Hence, the effect of cavity width on the SPL determined from their study was in contradiction to that reported by Block [4], although they did support Block's result that such cavities still maintain some tonal spectra at the lower velocities.

Although a number of prior investigations (including those stated above) have been conducted in order to gain an insight into the underlying physical behavior of cavity flows [7–18], differences in the state of the approaching boundary layer and L/W ratio have made it difficult to accurately predict the observed phenomena. Therefore, the goal of the present work was to systematically examine the effect of L/W on flow oscillations in an open cavity immersed in a turbulent boundary layer, for several different cavity widths, thereby assessing the three-dimensional nature of the cavity flowfield.

To accomplish this task an experimental program was undertaken using a single cavity model and several rectangular inserts that could be used to change the width and, therefore, the planform aspect ratio of the cavity. The present cavity was fabricated with an L/D of 1 and placed in a fully turbulent subsonic boundary layer flow where the effects of compressibility are negligible. This model was oriented such that its major axis was positioned perpendicular to the oncoming flow, thereby representing an open cavity configuration. At the lowest aspect ratio (L/W), quasitwo-dimensional results were obtained for this cavity model. The following sections provide details of this model and facility, as well as the results of the experimental program.

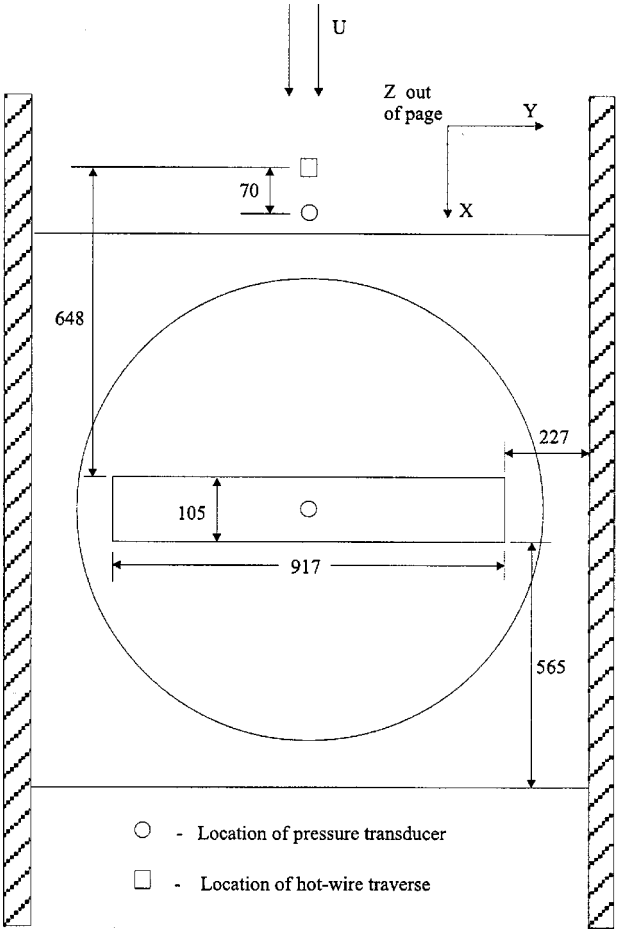

Fig. 2 Plan view of cavity model, turntable and transducer locations. (All dimensions in mm)

Experimental Approach

Wind Tunnel Facility and Cavity Model. This experimental program was carried out in a low speed, open circuit, boundary layer wind tunnel that has a rectangular working section of 1680 mm in height, 1370 mm in width, and 9000 mm in length, with a maximum freestream velocity of 25 m/s (Mach No. ~0.075) and a unit Reynolds number of $Re^*=1.75\times10^6\ m^{-1}$. A rectangular cavity model, constructed of plywood and masonite, was built within a turntable in the floor of the tunnel and positioned 7600 mm from the end of the wind tunnel contraction. This cavity has dimensions of 105 mm in length L as measured along its minor axis in the streamwise X direction, 917 mm in width W as measured in the spanwise Y direction, and 105 mm in depth D, see Fig. 1, giving initial geometrical conditions of $L/W=0.115$ and $L/D=1$. The model was positioned symmetrically across the tunnel, with the major axis perpendicular to the flow direction, such that the ends of the cavity were some 227 mm away from the side walls of the tunnel and outside the influence of the wall/floor corner vortices, see Fig. 2. The width of this model could be adjusted by placing a pair of tight fitting inserts into the cavity, one at each end, thereby effectively reducing the cavity width in a symmetrical manner. By this means, six different cavity widths were made available allowing six different planform ratios to be studied, as shown in Table 1.

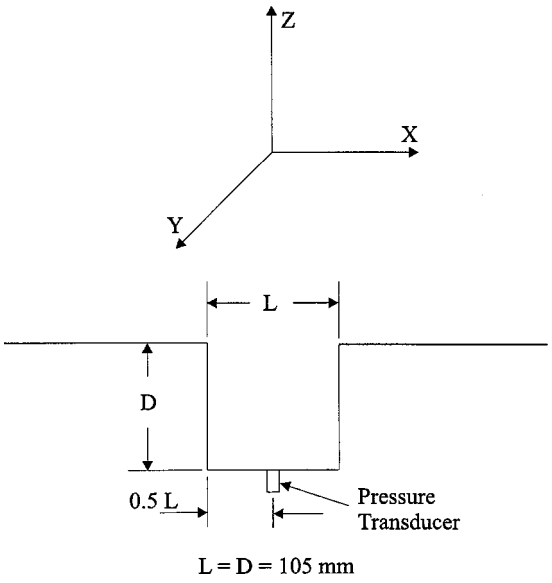

Fig. 1 Diagrammatic arrangement of cavity model cross section

Table 1 Geometries of the three-dimensional rectangular cavities

Cavity depth (D) mm			105			
Cavity length (L) mm			105			
Cavity width (W) mm	917	764	612	459	307	154
Planform ratio (L/W)	0.115	0.137	0.172	0.229	0.342	0.682

Instrumentation and Data Acquisition. Two different types of instrumentation were mainly used in this program, namely, hot-wire anemometry and omnidirectional condenser microphones. The hot wires were used for documenting the boundary layer and for determining its spectral energy at a specific height. The microphones were used as surface mounted pressure transducers to determine the spectral energy inside and outside the cavity.

The approaching boundary layer was checked for two dimensionality at five equally spaced spanwise locations 648 mm upstream from the cavity forward wall. In addition, a single hot wire was located in a similar upstream position, 5 mm above the floor, on the center line of the tunnel, for measurement of the spectral energy within the boundary layer. This was achieved by taking a time series for 20.64 s at a sampling rate of 16 kHz.

Unsteady pressures were acquired simultaneously at two locations, using the condenser microphones, with one unit positioned on the floor of the cavity at its geometric center and the other on the center line of the tunnel 578 mm upstream of the forward wall of the cavity. (This latter position was chosen so that the same model configuration can be used for future studies concerning effects of yaw of the cavity to the streamwise flow). All of the transducer signals were sampled over a period of 8 s at 25.6 kHz and analyzed using an HP 3562A dynamic signal analyzer, resolved over a frequency range from 10 Hz to 10 kHz, with the output being provided in the form of an energy spectrum $E(f)$. Data examined in the present study are based on an average of 50 such records, with each record consisting of 2048 samples. In order to determine the effect of the cavity width on the flow field the cavity spectra were normalized with respect to the upstream boundary layer spectrum.

In order that the true effects of changes in cavity width could be determined, it was necessary to first evaluate the effect of boundary layer disturbance as well as wind tunnel vibrations. This was achieved by analyzing the data from the upstream surface pressure transducer (microphone) as well as an accelerometer attached to the tunnel wall, in the absence of the cavity. Once these data were acquired the effect of cavity width with respect to length, in terms of planform aspect ratio L/W, could be ascertained. This was realized by recording the frequency and spectral energy of the flow oscillations for the different aspect ratios, using the surface pressure transducer in the floor of the cavity. The variance of the pressure signal was normalized by that measured by the upstream boundary layer pressure transducer to give a relative sound pressure level (RSPL) for each cavity width. In addition to the RSPL, the amplitude changes at given frequencies in the normalized spectra data were also determined.

Test Conditions. Throughout this series of tests the freestream velocity was maintained at 12.16 ± 0.1 m/s with a lateral uniformity of better than 2 percent, and a nominal turbulence intensity level of 0.28 percent, uniform to within 5 percent. Although the wind tunnel is configured as an open loop facility that exhausts into a very large laboratory, the temperature in the working section can rise several degrees centigrade over the period of an 8 h test. Therefore, the static temperature in the working section was monitored with a type T thermocouple and this was used to correct the freestream velocity. The uncertainty in the repeatability of the measurements of the static temperature and the hot-wire measurements were estimated to be ± 0.1°C and 1.5 percent, respectively. In addition, repeatability tests concerning specific microphone assemblies were carried out and these showed no measurable temperature effects on the performance of these devices.

Boundary layer traverses were made at five spanwise locations with a single hot-wire anemometer, with a positional accuracy of ± 0.004 mm. From these measurements the boundary layer thickness δ was estimated to be 210 mm, the displacement thickness δ_*, 18.3 mm, and the momentum thickness θ, 13.0 mm, giving a boundary layer shape factor H of 1.41. The Reynolds number based on the momentum thickness at this location was $\mathrm{Re}_\theta = 1.05 \times 10^4$, and the local skin friction coefficient and normalized friction velocity were determined from a Clauser plot analysis to be 0.0028 and 0.037, respectively [13]. The velocity profile data were replotted in terms of wall coordinates and compared with the law-of-the-wall, where good agreement was found to exist, implying that the approaching boundary layer was, indeed, a fully developed turbulent boundary layer. Furthermore, comparison of the hot-wire traverses acquired across the span of the tunnel revealed that the momentum thickness varied less than 9 percent across the tunnel width.

Results

Working Section Flow Oscillations. To ascertain the energy spectra of the boundary layer flow in the tunnel without the cavity being present, all the cavity inserts were installed within the cavity and this was then sealed from the flow. However, in order to provide a referencing system throughout this program, with and without the presence of the cavity, the transducer on the floor of the cavity remained active and capable of sensing the background noise as well as the tunnel vibrations. In this way, the boundary layer pressure fluctuations, as measured with the upstream transducer, were correlated to the cavity response by normalizing the boundary layer data against the sealed cavity data. The result of this analysis, referred to as the magnitude squared ratio (MSR), provided a normalized boundary layer energy spectrum, Fig. 3, in which a number of peaks in the frequency spectra were found. A similar analysis was also performed using a wall mounted accelerometer, again referenced to the cavity transducer, in order to separate the vibration and acoustic modes caused by the wind tunnel from the flow oscillation analysis. The energy spectrum, as shown in Fig. 3, provides evidence of seven clearly defined peaks, at 24.4, 42.2, 57.9, 141, 224, 258.5, and 365 Hz. Of these peaks the first five compared favorably with the frequency spectra acquired from the accelerometer and are thus considered to be due to mechanical vibration. The two large peaks at 258.5 and 365 Hz were not found in the spectra obtained using the accelerometer and, therefore, had to be accounted for.

The peak at 258.5 Hz was identified as the blade passing frequency since it was found that at the freestream value of 12 m/s, the rotational speed of the fan (317.5 rpm), together with the

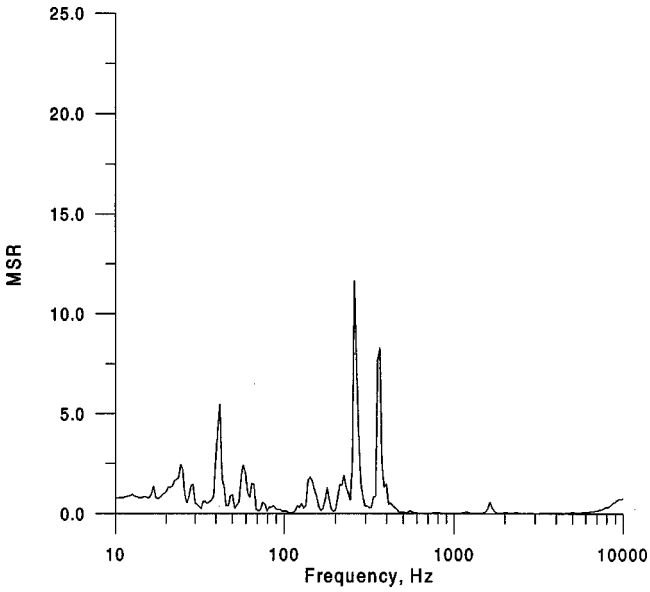

Fig. 3 MSR of boundary layer spectrum normalized by sealed cavity microphone spectrum

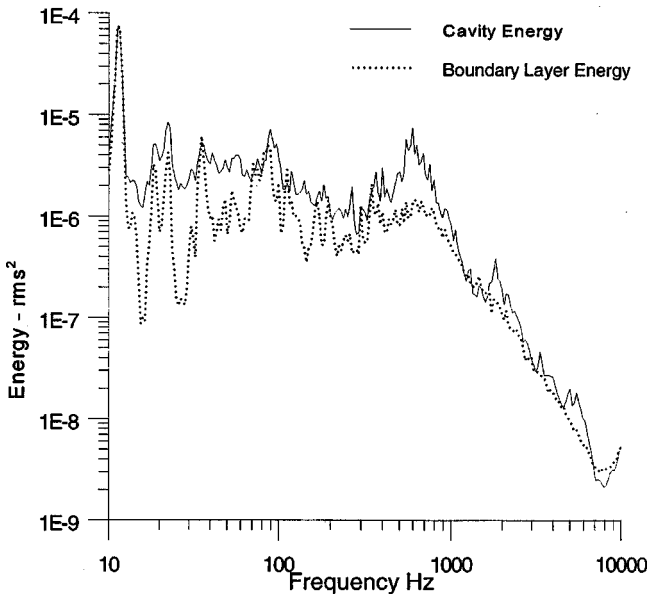

Fig. 4 Power spectral energy within the boundary layer $E(f)_B$ and the cavity $E(f)_C$

number of fan blades (48), provided a frequency of 254 Hz, a value comparable to the measured peak. However, the peak at 365 Hz could not be correlated so simply.

In an attempt to determine the source of this peak, the acoustic frequencies of the wind tunnel working section were approximated. This was achieved by evaluating the resonant acoustic frequencies of the working section from a simple expression typically used in the computation of enclosure or duct acoustics, namely,

$$f=\frac{c}{2}\left[\left(\frac{n_x}{L_{x*}}\right)^2+\left(\frac{n_y}{L_{y*}}\right)^2+\left(\frac{n_z}{L_{z*}}\right)^2\right]^{1/2} \tag{1}$$

where n_x, n_y, and n_z can independently take on integer values from 0,1,2, . . . ,∞, while L_{x*}, L_{y*}, L_{z*} are the corresponding geometrical dimensions of the working section and c is the local speed of sound. However, since the cavity microphone was located at the center of the cavity, only even integers could be correlated with this experiment. From this analysis it was found that several frequencies were within 10 percent of the observed peak at 365 Hz and, therefore, it was reasonable to assume that this frequency was, in fact, attributable to the working section acoustic response.

With the characteristics of the wind tunnel and boundary layer flow energy spectra now established it was possible to consider the energy spectra for the cavities of different widths. This was achieved by removing all the inserts from the cavity so that the largest planform was available, providing a cavity width of 917 mm, which gave a length to width ratio (L/W) of 0.115.

The turbulent boundary layer and cavity power spectra in the presence of the cavity flow are presented in Fig. 4. In order to be able to separate the cavity pressure fluctuations from the influence of tunnel oscillations, each cavity spectrum $E(f)_C$ was again, normalized by the energy spectrum $E(f)_B$ obtained simultaneously from the boundary layer transducer. This provided the magnitude (or amplitude) of the MSR and frequency content, over a frequency range from 10 Hz to 10 kHz, of the pressure oscillations resulting from the presence of the cavity. Typical values of these measurements are shown in Figs. 5(*a*) and 5(*b*) for two cavity L/W ratios: 0.115 and 0.682, respectively, these particular two being chosen because they represent the largest and the smallest planform ratios. The first three dominant peaks of the MSR were determined for each of the cavity configurations and are

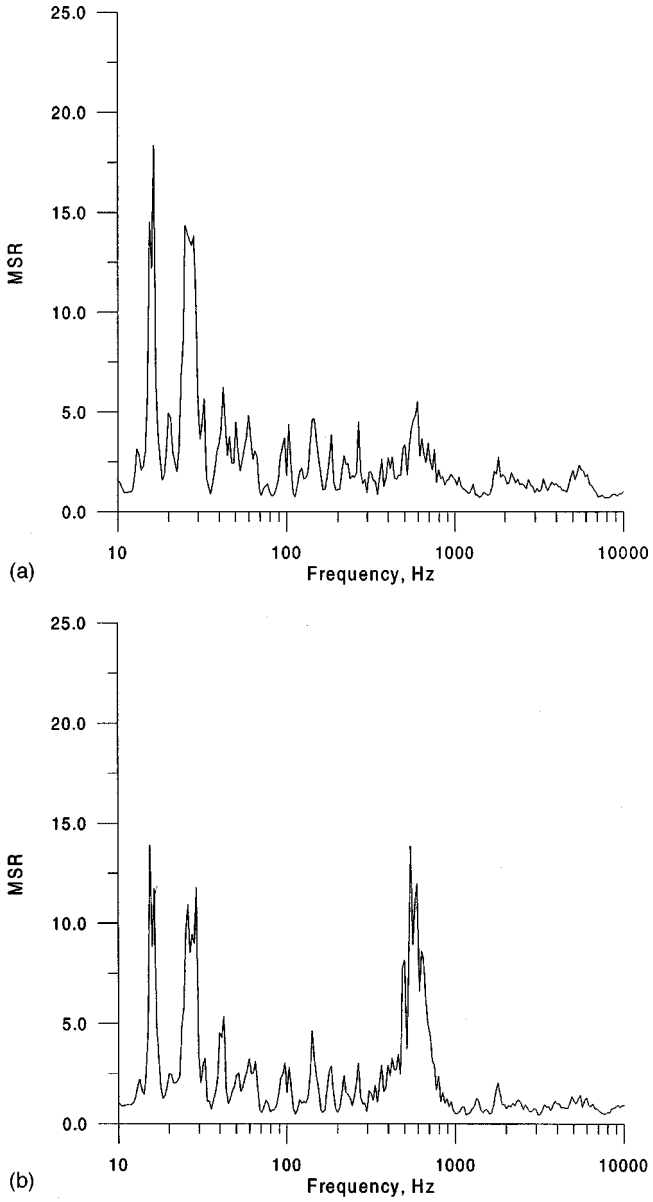

Fig. 5 (*a*) Ratio of the MSR of the cavity spectrum $E(f)_C$ to that of the boundary layer spectrum $E(f)_B$ for $L/W=0.115$. (*b*) Ratio of the MSR of the cavity spectrum $E(f)_C$ to that of the boundary layer spectrum $E(f)_B$ for $L/W=0.682$

presented in Table 2. It should also be noted that in some cases only two modes were capable of being readily detected. For example, in the case of the widest cavity ($L/W=0.115$), as shown in Fig. 5(*a*), two very strong peaks are observed at frequencies of 16 and 25 Hz, whereas for the narrowest cavity ($L/W=0.682$) shown in Fig. 5(*b*), three large peaks at 15, 29, and 546 Hz are evident.

In order to help to explain more fully the effect of the cavity within the boundary layer flow, the normalized spectral energy ratio (MSR) for the first three dominant modes versus L/W is presented in Figs. 6 and 7, while the RSPL for each L/W is presented in Fig. 8. These results are discussed in the next section.

In order to determine the SPL within a cavity the time histories of the surface pressures are used together with the expression

$$\mathrm{SPL}=10\log_{10}\left[\frac{(\overline{p'^2})_C}{20\times10^{-6}}\right] \tag{2}$$

Table 2 Variation of peak frequencies in the different cavities

Cavity width (mm)	*L/W* ratio	First largest MSR peak		Second largest MSR peak		Third largest MSR peak	
		Frequency (Hz)	MSR	Frequency (Hz)	MSR	Frequency (Hz)	MSR
917	0.115	16	18.4	25	14.4	546	5.4
764	0.137	15	24.5	29	20	546	5.0
612	0.172	28	19.3	16	15.6	546	5.4
459	0.229	16	18.9	27	16.2	546	7.3
307	0.342	15	16.3	28	12.4	546	10.2
154	0.682	15	13.9	546	13.9	29	11.8

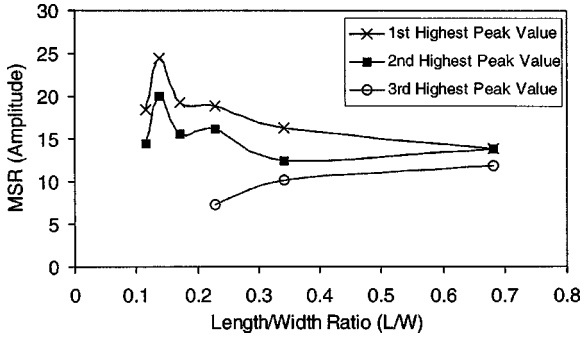

Fig. 6 MSR of three most dominant peaks (in terms of amplitude) as a function of *L/W*

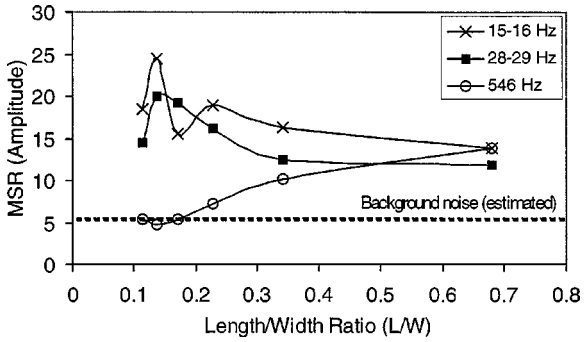

Fig. 7 MSR of three most dominant peaks (at constant frequency) as a function of *L/W*

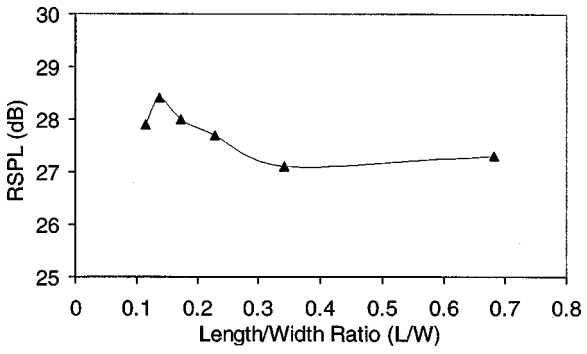

Fig. 8 Relative sound pressure level as a function of *L/W*

where 20×10^{-6} Pa is the standard reference values used in acoustics and p' represents the fluctuating component of the pressure p, given by

$$\overline{p'^2}=\frac{1}{F}\int_{f_1}^{f_2}(p-\overline{p})^2 df \tag{3}$$

where F is defined as the frequency interval f_2-f_1.

However, in order to determine the effect of L/W related to the upstream conditions, that is the boundary layer, and, thereby, ascertain whether the total energy for each L/W was merely redistributed or if the total energy contained within the cavity actually increased, a RSPL was calculated. This was determined from the following expression and the results are shown in Fig. 8

$$\mathrm{RSPL}=10\log_{10}\overline{\left(\frac{(p'^2)_C}{(p'^2)_B}\right)}. \tag{4}$$

Therefore, the values calculated using this equation provide direct information concerning the relative change in the SPL resulting from the addition of the cavity, as well as changes due to modifications of the cavity geometry. Furthermore, by using a sound level meter, a baseline sound level (dB) in the absence of the cavity was recorded and, under the present test conditions, this value was determined to be approximately 75 dB.

Discussion

The experimental results obtained from the two microphone transducers have highlighted a number of areas of interest and may help to provide further insight into the effect of cavity flows in subsonic boundary layers. In particular, the pressure oscillations that are set up due to the presence of a cavity within a relatively thick boundary layer are clearly dependent on cavity width. This effectively influences (a) the frequency of oscillations, (b) the spectral energy contained within the flow oscillations, and (c) the sound pressure level generated by the cavity. These aspects are discussed in the following sections.

Effect of Cavity Width on the Frequency of the Oscillations. In order to discuss the manner in which changes in cavity width may affect pressure oscillations when a cavity is subjected to a boundary layer flow, it is constructive to first observe the results given Table 2. From graphical observations of the MSR against frequency, for each of the six L/W ratios, similar to those shown in Figs. 5(*a*) and 5(*b*), the dominant peaks were ascertained. However, since it was expected from geometrical considerations that only acoustic frequencies of less than 1000 Hz could be attributable to this size and shape of cavity in a subsonic flow, a maximum of three peaks were examined. Therefore, Table 2 provides the values of the frequency and the MSR for the three dominant peaks for each of the six cavity models.

The first observation to make from this table is that for L/W ratios of less than 0.172 only two dominant peaks occur (see Fig. 5(*a*)), whereas for L/W ratios greater than 0.229, three dominant peaks are evident (see Fig. 5(*b*)). Furthermore, for L/W ratios between 0.115 and 0.342 the frequencies of the first and second highest peaks are approximately constant at 16 and 28 Hz, respectively, except for the $L/W=0.172$ case. Here, the dominant peaks have ''switched'' values with the first dominant peak at 28 Hz and the second peak at 16 Hz.

With increasing L/W ratio (reduction in cavity width) between 0.229 and 0.682, a third peak becomes more noticeable at the higher frequency of 546 Hz. The amplitude at this particular frequency increases as L/W increases, so much so that at L/W

$=0.682$ (the smallest cavity width) this frequency has the second highest MSR value and is similar in amplitude to the first dominant peak (MSR=13.9). What was nominally the second dominant peak at approximately 28 Hz for an L/W of 0.342 is then reduced to become the third peak with a MSR of 11.8 at 29 Hz for the highest L/W ratio.

In order to appreciate the changes that take place as the cavity width is decreased, Fig. 6 shows how the MSR varies with increasing L/W for the three different dominant peak values, with both the first and second dominant peaks closely following one another. However, because the ordering of the peaks in the frequency domain changes, this figure does not show how the peaks at specific frequencies are varying. If these results are presented as changes in MSR with increasing L/W for constant frequencies of 15–16, 28–29, and 546 Hz, Fig. 7, a more detailed picture emerges. In this case it can be seen that the 16 Hz, low frequency, pressure oscillation peaks at a MSR of 24.5 for a L/W of 0.137, and is then quickly attenuated as L/W increases to 0.172. The peak recovers some energy as L/W increases further, but then reduces at higher L/W ratios. The peak at the second dominant frequency of 28 Hz is much more consistent. Here, the energy is contained below an MSR of 20 but maintained over a range of L/W ratios between approximately 0.137 and 0.229 before, once more, reducing as L/W increases. Although the third and highest frequency of 546 Hz is not as noticeable for cavities that have widths greater than four times the cavity length, it is still observable, but buried within the background noise, Figs. 5(*a*) and 7. However, for values of L/W above 0.229 the energy at this frequency rises with increasing L/W, Fig. 7.

In order to attempt to explain the nature of these oscillations the acoustic modes of the cavity model were considered. Clearly, the source of the peak is not related to a cavity width mode, although changes in width do affect the magnitude of the peak. From experiments using cavity models with L/W ratios from 0.053 to 0.162 and L/D ratios from 0.12 to 1.17, East [5] showed that there was a functional relationship between the acoustic normal depth mode Strouhal number $(=fD/c)$ and L/D

$$\mathrm{St}=\frac{fD}{c}=\frac{1}{4\left(1+0.65\left(\frac{L}{D}\right)^{0.75}\right)}. \tag{5}$$

This shows that the Strouhal number increases as L/D decreases, giving an asymptotic value of about 0.25 for very narrow cavities $(L/D\sim 0)$. This empirical expression agrees well with the theoretical prediction curves of Plumblee et al. [3] and Tam [9].

For the present case of $L/D=1$ the predicted value of St is 0.152 ± 0.015, taking into account the scatter in the data of East [5]. The frequency of 546 Hz gives a Strouhal number of 0.165 which is within the predicted range, indicating that this peak is associated with a depth mode acoustic response.

Spectral Energy Content of the Flow Oscillations. The energy associated with a given frequency of oscillation may be referred to as the spectral energy and this may be related to the MSR obtained from the signal analyzer. From observations of the change in MSR with L/W ratio for a given frequency, Fig. 7, it can be seen that there appears to be a switch in the amount of energy between the two low frequency oscillations, namely the 16 and 28 Hz frequencies. (This would occur at approximate L/W ratios of 0.15 and 0.20, respectively, and is probably related to cavities that have a width more than five times the cavity length.) The energy contained within these low frequency oscillations is produced by the fluid dynamic process caused by the presence of the cavity and is dominant for large width cavities. However, as the cavity width is reduced (increasing L/W) the energy contained in these frequencies tends to attenuate to a near constant value, whereas the energy in the acoustic oscillations appears to increase in magnitude, Fig. 7. From this, it may be surmised that, as the cavity width is further reduced beyond the range examined here, the acoustic energy would increase and dominate over that produced by the fluid flow oscillations.

The results of this analysis pose the question that if the energy provided by the fluid oscillations remains relatively constant as the cavity width is further reduced and the energy provided by the acoustic oscillations is increasing, then where does this apparent increase in spectral energy come from? In order to answer this question and gain an understanding of the process involved, the total energy must be estimated, and this was accomplished by calculating a RSPL for the six cavities.

Variation of RSPL With Cavity Width. Although a particular frequency may be enhanced as L/W is changed, inspection of Fig. 8 clearly shows that the values of the RSPL range between 27 and 28.5 dB, having variations of less than 1.5 dB. Even though this change in dB level at first appears to be small, it must be remembered that dB is logarithmic and, therefore, such a variation in dB can be equated to an energy change of approximately 40 percent. In this particular case, the cavity with $L/W=0.137$ gives the maximum RSPL and, since, within the range examined, the acoustic energy is greatest at the largest L/W (that is 0.682), the maximum RSPL appears to relate cavity unsteadiness to a state of fluid dynamic resonance. In addition, as the L/W ratio increases (decreasing width of cavity) the RSPL tends toward an asymptote, similar to that found by Ahuja and Mendoza [6]. In general, the levels of the fluid dynamic oscillation found for these six cavities are greater than the acoustic oscillations.

From the above information it is apparent that although some energy may have been transferred from one frequency to another, an increase in total energy obtained from the mean flow must have also occurred. Although previous researchers have considered that the shear layer spanning the cavity provided the energy responsible for cavity oscillations, the source of this energy is disputed. Plumbee et al. [3] suggested that the energy was a result of broadband turbulence, while Tam and Block [10] believed that the shear layer instabilities were the source. The present authors examined the upstream boundary layer dissipation spectra and determined that the region of maximum dissipation occurs between 650 and 850 Hz. Within this region energy is directly dissipated by viscous forces. Therefore, it is highly unlikely that sufficient energy is available to excite the cavity fluid dynamically in this range. Hence, the present study offers little support for the Plumbee et al. [3] model at low L/W values, and tends to support the Tam and Block [10] hypothesis of shear layer instability as the mechanism for energy transfer to the cavity. This is possible because of the large availability of energy in the boundary layer in the low frequency range [13]. The large vortical motions which occupy the low frequency range of the spectra (less than 100 Hz) contain energy levels two orders of magnitude higher than the eddies in the dissipation region. It is, therefore, likely that some of this energy would be available for coupling to cavity oscillations. In addition, as the width of the cavity is decreased (L/W increased), the region of maximum boundary layer dissipation approximately coincides with the frequency of the acoustic oscillations within the cavity. This liberation of boundary layer energy appears to support the growth of the natural acoustic frequencies predicted using Eq. (5). Although the source of this energy may be related to the smaller scales of motion and is, therefore, short lived, sufficient energy is apparently available to enable the growth of these acoustic oscillations. Indeed, although it may be expected that when the energy of the acoustic and the fluid dynamic oscillations coincide the resulting amplitude could become quite large (a result that has been observed in supersonic cavity flows [13]), this was not observed for the present geometry.

Summary

An experimental investigation of the flow oscillations created by a rectangular cavity of varying width has been undertaken. This cavity, with an L/D of unity, was immersed in a thick tur-

bulent boundary layer in subsonic flow, and the planform aspect ratio (L/W) for six cavities was varied from 0.115 to 0.682. Unsteady pressure measurements were taken with omnidirectional microphones in both the boundary layer and within the cavity, which was set with its principal axis normal to the freestream direction. The frequencies of oscillations produced by the wind tunnel in the absence of the cavity were determined, with mechanical oscillations being measured using an accelerometer attached to the tunnel wall and flow oscillations by the surface mounted microphones. From an analysis of the ratio of the unsteady pressures within the cavity to those of the upstream boundary layer it was found that:

(a) The number of dominant frequencies increased as the width of the cavity was reduced, that is, as the length/width ratio (L/W) decreased. It was found that for cavities with widths of more than four times the cavity length, fluid flow oscillations were prevalent with two pronounced specific frequencies, whereas with smaller cavities a third large oscillation occurs that is acoustically driven.

(b) There appears to be a ''switch'' in the amount of energy between the low frequencies as the cavity width is decreased for the larger cavities, whereas there is a steady increase in the acoustic energy for cavities of widths less than four times the cavity length.

(c) The relative sound pressure level appears to relate much of the cavity unsteadiness to a state of fluid dynamic resonance rather than acoustic resonance. This was shown to occur for the larger width cavities and produced variations in the RSPL of 1.5 dB, which could be equated to a 40 percent energy increase due to the presence of the cavity.

Acknowledgments

The authors wish to thank the University of Cincinnati for providing Dr. Disimile with academic leave in England, and the University of Surrey for providing wind tunnel time and technical support. In addition, the authors greatly appreciate the engineering support of Curtis W. Fox.

Nomenclature

c = local speed of sound within the freestream (m/s)
D = depth of the cavity (mm)
$E(f)$ = spectral energy (rms^2)
f_v = vortex shedding frequency (Hz)
F = frequency range between f_1 and f_2
H = boundary layer shape factor
L = length of the cavity, the dimension along the minor axis (mm)
L/D = length to depth ratio of the cavity
L/W = planform aspect ratio of the cavity
L_{x*}, L_{y*}, L_{z*} = characteristic working section dimensions in the X, Y, and Z directions (mm)
MSR = magnitude squared ratio $(E(f)_C/E(f)_B)$
n_x, n_y, n_z = acoustic mode number used in duct resonance equation ($n=1,2,3,\ldots$)
p = instantaneous pressure component
$\overline{p}$ = average pressure over a time period
p' = fluctuating pressure component
Q = quality factor (ratio of the center frequency/bandwidth of the peaks)
RSPL = relative sound pressure level (dB)
Re* = unit Reynolds number (m^{-1})
Re_θ = Reynolds number based on the momentum thickness
St_θ = Strouhal number based on the momentum thickness ($f_v\theta/U_\infty$)
U_∞ = freestream velocity (m/s)
W = width of the cavity, the dimension along the major axis (mm)
X,Y,Z = streamwise, spanwise, and transverse spatial coordinates (mm)
δ = boundary layer thickness defined by 99.5 percent of freestream velocity (mm)
δ_* = boundary layer displacement thickness (mm)
θ = boundary layer momentum thickness (mm)

Subscripts

B = boundary layer transducer
C = cavity transducer

References

[1] Rockwell, D., and Naudascher, E., 1979, ''Self-Sustained Oscillations of Impinging Free Shear Layer,'' Annu. Rev. Fluid Mech., **11**, pp. 67–94.
[2] Rossiter, I. E., 1966, ''Wind Tunnel Experiments on the Flow Field over Rectangular Cavities at Subsonic and Transonic Speeds,'' Aeronautical Research Council, R&M Report No. 3438.
[3] Plumblee, H. E., Gibson, J. S., and Lassiter, L. W., 1962, ''A Theoretical and Experimental Investigation of the Acoustic Response of Cavities in Aerodynamic Flow,'' Report No. WADD TR-61-75, Wright-Patterson Air Force Base, Dayton, Ohio.
[4] Block, P. J. W., 1976, ''Noise Response of Cavities of Varying Dimensions at Subsonic Speeds,'' NASA Report No. TN D 8351.
[5] East, L. F., 1966, ''Aerodynamically Induced Resonance in Rectangular Cavities,'' J. Sound Vib., **3**, pp. 277–287.
[6] Ahuja, K. K., and Medoza, J., 1995, ''Effects of Cavity Dimensions, Boundary Layer, and Temperature on Cavity Noise with Emphasis on Benchmark Data to Validate Computational Aeroacoustic Codes,'' NASA Contractor Report No. 4653.
[7] Karamcheti, K., 1955, ''Acoustic Radiation from Two-Dimensional Rectangular Cutouts in Aerodymanic Surfaces,'' NACA Report No. TN 3487.
[8] NASA Tech. Briefs, 1996, ''Study of Airflow Tangential to a Screen,'' ARC-13213, Ames Research Center.
[9] Tam, C. K. W., 1976, ''The Acoustic Modes of a Two-Dimensional Rectangular Cavity,'' J. Sound Vib., **49**, pp. 353–364.
[10] Tam, C. K. W., and Block, P. J. W., 1978, ''On the Tones and Pressure Oscillations Induced by Flow over Rectangular Cavities,'' J. Fluid Mech., **89**, pp. 373–399.
[11] Komerath, N. M., Ahuja, K. K., and Chambers, F. W., 1987, ''Prediction and Measurement of Flows over Cavities — A Survey,'' *AIAA-87-0166, 25th Aerospace Sciences Meeting*, Reno, NV, January 12–15.
[12] Disimile, P. J., DiMicco, R. G., Lueders, K., Savory, E., and Toy, N., 1990, ''Unsteady flow in a Three-Dimensional Rectangular Cavity Immersed in a Subsonic Crossflow,'' *ASME Conference, Forum on Unsteady Flow*, Vol. 102, Atlanta, Georgia, pp. 45–50.
[13] Disimile, P. J., Toy, N., and Savory, E., 1998, ''Pressure Oscillations in a Subsonic Cavity at Yaw,'' AIAA J., **36**, pp. 1141–1148.
[14] Tracy, M. B., Plentovich, E. B., and Chu, J., 1992, ''Measurements of Fluctuating Pressure in a Rectangular Cavity in Transonic Flow at High Reynolds Numbers,'' NASA Report No. TM 4363.
[15] Savory, E., Toy, N., Disimile, P. J., and DiMicco, R. G., 1993, ''The Drag of Three-Dimensional Rectangular Cavities,'' J. Appl. Sci. Res., **50**, pp. 325–346.
[16] Tam, C. J., Orkwis, P. D., and Disimile, P. J., 1996, ''Algebraic Turbulence Model Simulations of Supersonic Open Cavity Flow Physics,'' AIAA J., **34**, pp. 2255–2260.
[17] Disimile, P. J., and Orkwis, P. D., 1997, ''Effect of Yaw on the Frequency of Pressure Oscillations within a Rectangular Cavity at Mach 2,'' AIAA J., **35**, pp. 1233–1235.
[18] Disimile, P. J., and Orkwis, P. D., 1998, ''Sound Pressure-Level Variations in a Supersonic Rectangular Cavity at Yaw,'' J. Propul. Power, **14**, pp. 392–398.